ACSNANO
www.acsnano.org
ARTICLE

All-Optical Chirality-Sensitive Sorting *via* Reversible Lateral Forces in Interference Fields

Tianhang Zhang,[†,‡] Mahdy Rahman Chowdhury Mahdy,[‡,§] Yongmin Liu,[∥] Jing Hua Teng,[⊥] Chwee Teck Lim,[†,#] Zheng Wang,[¶] and Cheng-Wei Qiu*[,†,‡]

[†]Graduate School for Integrative Sciences and Engineering, National University of Singapore, Centre for Life Sciences (CeLS), #05-01, 28 Medical Drive, Singapore 117456, Singapore

[‡]Department of Electrical and Computer Engineering and [#]Department of Biomedical Engineering, National University of Singapore, 4 Engineering Drive 3, Singapore 117583, Singapore

[§]Department of Electrical & Computer Engineering, North South University, Bashundhara, Dhaka 1229, Bangladesh

[∥]Department of Mechanical and Industrial Engineering, Department of Electrical and Computer Engineering, Northeastern University, Boston, Massachusetts 02115, United States

[⊥]Institute of Materials Research and Engineering, Agency for Science Technology and Research (A*STAR), #08-03, 2 Fusionopolis Way, Innovis 138634, Singapore

[¶]Department of Electrical and Computer Engineering, University of Texas at Austin, 2501 Speedway, Austin, Texas 78712, United States

Supporting Information

ABSTRACT: **Separating substances by their chirality faces great challenges as well as opportunities in chemistry and biology. In this study, we propose an all-optical solution for passive sorting of chiral objects using chirality-dependent lateral optical forces induced by judiciously interfered fields. First, we investigate the optical forces when the chiral objects are situated in the interference field formed by two plane waves with arbitrary polarization states. When the plane waves are either linearly or circularly polarized, nonzero lateral forces are found at the particle's trapping positions, making such sideways motions observable. Although the lateral forces have different magnitudes on particles with different chirality, their directions are the same for opposite handedness particles, rendering it difficult to separate the chiral particles. We further solve the sorting problem by investigating more complicated polarization states. Finally, we achieve the chiral-selective separation by illuminating only one beam toward the chiral substance situated at an interface between two media, taking advantage of the native interference between the incident and reflective beams at the interface. Our study provides a robust and insightful approach to sort chiral substances and biomolecules with plausible optical setups.**

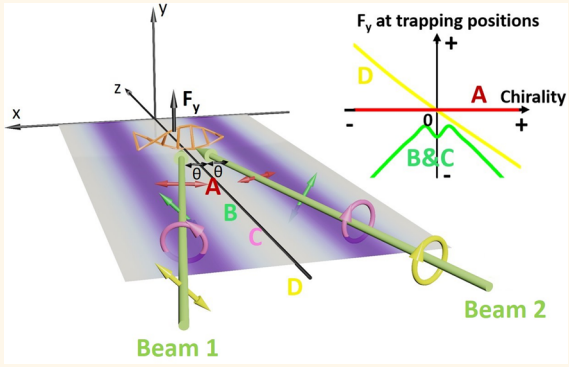

KEYWORDS: *optical forces, lateral forces, chirality, separating, interference field, interface*

In a highly focused laser beam, an illuminated particle could experience a restoring force pointing toward the focal point with magnitude proportional to the optical field gradient, *i.e.*, gradient force. The optical tweezers[1] based on this force has been developed into a very powerful tool to trap varieties of materials in a microscopic system and has found numerous applications in the fields of biological science,[2−4] chemistry,[5,6] physics,[7,8] and engineering.[9,10] On the other hand, light carrying orbital angular momentum[11] could exert nonconservative force on an illuminated object through the momentum transfer. Intuitively, the nonconservative force should always be along the beam propagating direction. More recently, it has been found that the direction of the nonconservative force could be opposite[12−16] or perpendicular[17,18] to the light propagation direction, by using judiciously structured light illumination. An intuitive perception is that the degree of freedom empowering such fascinating phenomena resides in either the structuring complexity of light or material sophistication, or a combination of both parties.

Received: February 28, 2017
Accepted: April 2, 2017
Published: April 2, 2017

DOI: 10.1021/acsnano.7b01428
ACS Nano 2017, 11, 4292−4300

Chirality refers to the property of a structure that is nonsuperimposable with its mirror image. In chemistry, the image pairs of a chiral molecule are called enantiomers, while individual enantiomers exhibit left-handed or right-handed chirality. The identification and separation of chiral substances always represent a research topic drawing wide interest in chemistry: chiral pesticides may exhibit differences in environmental activity and persistence;[19] chiral fragrance may elicit different notes.[20] Arguably the most important application of chirality identification and separation is in the pharmaceutical industry since individual enantiomers of chiral drugs may have very different bioactivities and biotoxicities.[21] Worldwide sales of chiral drugs in single-enantiomer forms increased continuously from $74.4 billion in 1996 to $225 billion in 2005. Meanwhile chiral separations have been considered among the most difficult separations in analytical chemistry.[22] Usually, reagents or microorganisms are introduced to salinize both of the enantiomers or enzymatically assimilate one of them. Appropriate reaction agents and methods have to be found for separations of each type, which greatly enhanced the overall complexity. On the other hand, recent studies have proposed and demonstrated noninvasive alternatives to separate chiral objects by optical method.[23−26]

Chiral objects with the opposite handedness tend to interact differently with the chiral environments. The chirality of light (related to the spin angular momentum)[27,28] has been studied to design chiral metamaterials[29−31] and sense chiral molecules.[32−34] It could also be another native degree of freedom to explore optical micromanipulation for chiral objects. By properly tailoring the light interaction with chiral objects, a force (usually termed *lateral force*) is predicted when the object is placed above a slab[24] or in an evanescent wave.[25] The chiral particle is trapped near the surface by the field gradient and pushed in the field propagating direction. Other than these two forces, the lateral force arises due to the transverse spin angular momentum carried by the field, and its direction is perpendicular to both the field propagating direction and the field gradient direction. However, the field is restricted very near the surface, which results in limited lateral forces on chiral objects with large sizes. Chen *et al.* investigated the optical forces on a chiral object when it is placed in the interference field formed by two p-polarized plane waves, which refers to case A in Figure 1a.[35] Although the lateral force arises at some positions, the lateral force is always zero at the object's equilibrium positions determined by the trapping force. This may result in a consequence that the particle would be eventually trapped and pushed in the forward direction, but the lateral force would thus vanish as marked in Figure 1b.

In this work, we demonstrate an approach to separate chiral objects with a size from the nanometer scale to the micrometer scale using lateral forces induced in the interference field. First, we explore the possibility of separating chiral particles when they are placed in the interference field formed by two plane waves. We find that the polarization states of those two interfering beams play sophisticated roles in producing the lateral force at the particle's trapping positions. When the polarization states of two waves are both linear, nonzero lateral forces are found at the trapping positions when the polarization direction is not completely horizontal (s) or vertical (p), referring to case B in Figure 1a, making the sideways motions observable. As the chirality of the objects increases, both the trapping force and lateral force are phase shifted due to the combined effect of the transverse orbital angular momentum[18]

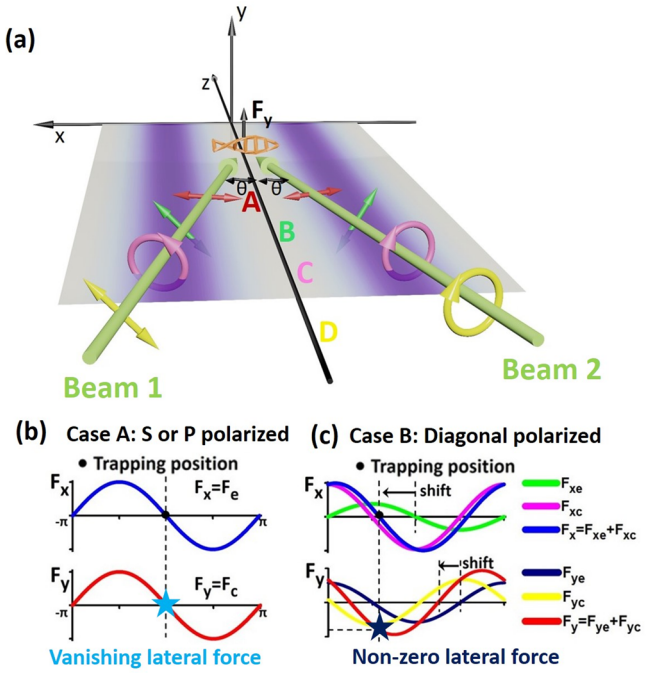

Figure 1. (a) Schematic of interference fields investigated in the current paper: the four cases under study with different polarization states are marked by A, B, C, and D. (b) In case A, the trapping force and lateral force are completely in phase, making the lateral force at the trapping position always zero. (c) In case B, both the trapping force and the lateral force shift when the object shows chirality, as a result the trapping force and lateral force not being completely in phase. The lateral forces at the trapping position are not zero but in the same direction for chiral objects with opposite handedness (refer to Figures 2 and 3). F_e and F_c represent the nonchiral and chiral portion of the force, respectively. In case C, the lateral forces at the trapping position are not zero but also in the same direction for chiral objects with opposite handedness similar to case B (refer to section 4.3 in the Supporting Information). In case D, the lateral forces at the trapping position are not zero and in the opposite directions for chiral objects with opposite handedness (refer to Figure 4). There are multiple trapping positions in the interference field, while one trapping position within a single period is plotted in (b) and (c).

and transverse spin angular momentum. Such shifts make the lateral force at the new trapping position nonzero, as marked in Figure 1c. Although these forces may be helpful for discriminating objects with chirality of the same sign but different values, the lateral force has the same sign on a chiral particle with opposite handedness, making the separating process difficult to distinguish. When the polarization states are both circular (case C in Figure 1a), the lateral forces at the trapping positions are similar to those of case B. To solve the separation problem, we have investigated more sophisticated polarization states. We find that when one of the incident beams is linear polarized and the other one is circularly polarized, the phase shift of the trapping force is insensitive to the chirality, while that of the lateral force is sensitive, which leads to a chirality-sensitive lateral force separating chiral particles with opposite handedness. Finally, we implement the separation by illuminating a single beam with the degrees of freedom brought by the interference. We place the chiral objects at an interface between two media and take advantages of the incident-reflection waves formed by the interference field to induce the lateral force. The lateral force is also sensitive to

DOI: 10.1021/acsnano.7b01428
ACS Nano 2017, 11, 4292−4300

both the direction and value of the chirality and insensitive to the particle's position, making the sorting process robust. The separation is not restricted to nanometer-scale objects but is also applied to micrometer-scale objects.

RESULTS AND DISCUSSION

Analytical Derivation of Optical Forces on Chiral Dipoles. To illustrate the lateral force, we model the chiral object as a chiral dipole and analytically write the optical force when it is placed in the interference field consisting of two plane waves as shown in Figure 2a. The relationships between

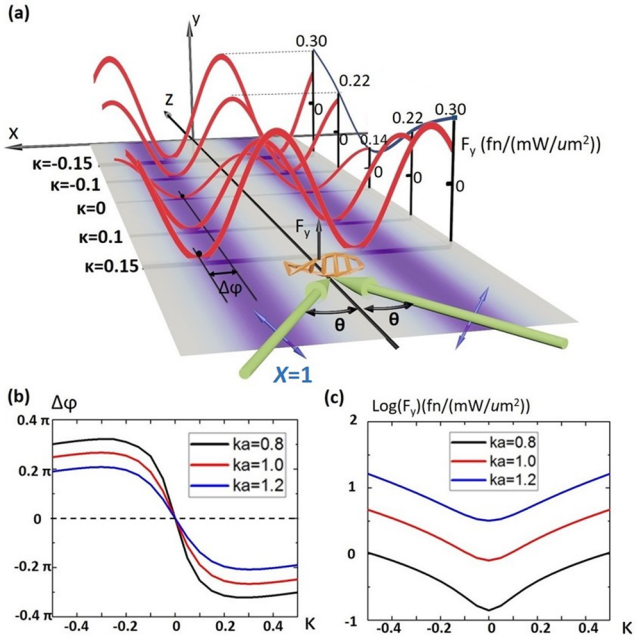

Figure 2. (a) Lateral force on a chiral object in an interference field consisting of two plane waves propagating in angles $+\theta$ and $-\theta$ with the z-axis in a mirror diagonal polarization state (case B): as can be seen in eqs 12 and 13, the lateral force is always in sinusoidal form. φ is defined as the phase of the lateral force and F_y is defined as the amplitude of the lateral force. Both the phase and magnitude of the lateral force F_y change when varying the object's chirality. $\Delta\varphi$ is defined as the phase shift with respect to nonchiral particles. The lateral force's (b) phase shift and (c) amplitude in log scale when varying the particle's chirality parameter κ when ka = 0.8, 1, and 1.2. The incident angle θ is set to 10 degrees. Spherical chiral particles with ε_r = 2.1, u_r = 1, and chirality parameter κ are considered.

the induced electric ($\mathbf{p}$) and magnetic momentum ($\mathbf{m}$) and the external field for chiral dipoles are described by the constitutive relations.[36]

$$\mathbf{p} = \alpha_e \mathbf{E} + i\chi \mathbf{H}$$
$$\mathbf{m} = -i\chi \mathbf{E} + \alpha_m \mathbf{H} \quad (1)$$

Besides the complex electric polarizability α_e and the magnetic polarizability α_m, the complex chiral polarizability χ is also introduced in the relations. α_e, α_m, and χ are complex functions of the relative permittivity ε_r, the relative permeability μ_r, and the chirality parameter $\kappa \in [-1, 1]$. The chiral material properties defined by ε_r, μ_r, and κ are shown in the Methods. Both κ and χ are set to zero for particles without chirality and reverse their signs for objects with opposite handedness. The time-averaged optical force (detailed derivation in the Methods) is given by

$$\langle \mathbf{F} \rangle = \langle \mathbf{F}_{EM} \rangle + \langle \mathbf{F}_{INT} \rangle \quad (2)$$

$$\langle \mathbf{F}_{EM} \rangle = \frac{\mathrm{Re}[\alpha_e]}{\varepsilon_0 \varepsilon_b} \nabla \bar{W}_e + \frac{\mathrm{Re}[\alpha_m]}{\mu_0 \mu_b} \nabla \bar{W}_m + \frac{2\omega \mu_b}{\varepsilon_0} \mathrm{Im}[\alpha_e] \bar{\mathbf{P}}_e^o + \frac{2\omega \varepsilon_b}{\mu_0} \mathrm{Im}[\alpha_m] \bar{\mathbf{P}}_m^o + c\,\mathrm{Re}[\chi] \nabla \bar{K} + \mathrm{Im}[\chi](2\omega^2 \mathbf{S} - c^2 \nabla \times \bar{\mathbf{P}}) \quad (3)$$

$$\langle \mathbf{F}_{INT} \rangle = -\frac{c^3 k^4}{6\pi} \left((\mathrm{Re}[\alpha_e \alpha_m^*] + |\chi|^2) \bar{\mathbf{P}} - \frac{1}{2c^2} \mathrm{Im}[\alpha_e \alpha_m^*] \mathrm{Im}[\mathbf{E} \times \mathbf{H}^*] \right) - \frac{c^2 k^5}{3\pi} \left(\frac{\mu_b}{\varepsilon_0} \mathrm{Re}[\alpha_e \chi^*] \mathbf{S}_e + \frac{\varepsilon_b}{\mu_0} \mathrm{Re}[\alpha_m \chi^*] \mathbf{S}_m \right) \quad (4)$$

where $\mathbf{E}$ and $\mathbf{H}$ are the incident electric and magnetic field vector. ε_b, μ_b, ω, and k are the relative permittivity, the permeability of the background, the angular frequency, and wavenumber of light, respectively. The time-averaged optical force is separated into the dipole part $\mathbf{F}_{EM}$, representing the contributions from the electric dipole and the magnetic dipole, and the interaction part $\mathbf{F}_{int}$, representing the contributions from the direct interaction between the electric and magnetic dipoles. $\bar{W}_e = \frac{1}{4}\varepsilon_0 \varepsilon_b |\mathbf{E}|^2$, $\bar{W}_m = \frac{1}{4}\mu_0 \mu_b |\mathbf{H}|^2$, and $\bar{K} = \frac{1}{2c}\mathrm{Im}[\mathbf{E} \cdot \mathbf{H}^*]$ are the electric and magnetic component of the time-averaged energy density and the chirality density. The gradient of these three terms multiplied by the active part of the polarizability coefficients gives the gradient force. The momentum density $\bar{\mathbf{P}}$ could be separated into the orbital part $\bar{\mathbf{P}}^o$ and the spin part $\bar{\mathbf{P}}^s$, where

$$\bar{\mathbf{P}} = \frac{\mathrm{Re}[\mathbf{E} \times \mathbf{H}^*]}{2c^2}$$
$$\bar{\mathbf{P}}_e^o = -\frac{\varepsilon_0}{4\omega \mu_b} \mathrm{Im}[\mathbf{E}(\nabla \otimes \mathbf{E}^*)]$$
$$\bar{\mathbf{P}}_m^o = -\frac{\mu_0}{4\omega \varepsilon_b} \mathrm{Im}[\mathbf{H}(\nabla \otimes \mathbf{H}^*)]$$
$$\bar{\mathbf{P}}^s = \frac{1}{2} \nabla \times \left(-\frac{\varepsilon_0}{4\mu_b \omega i} \mathbf{E} \times \mathbf{E}^* - \frac{\mu_0}{4\varepsilon_b \omega i} \mathbf{H} \times \mathbf{H}^* \right) \quad (5)$$

The orbital part $\bar{\mathbf{P}}^o = \bar{\mathbf{P}}_e^o + \bar{\mathbf{P}}_m^o$ represents the "the directly observable momentum of light".[17,18] The spin part $\bar{\mathbf{P}}^s$ has a transverse component in the evanescent field and interference field; thus it is essential to producing the lateral force for nonchiral particles in previous cases.[17,18] The spin angular momentum $\mathbf{S}$ where

$$\mathbf{S} = \mathbf{S}_e + \mathbf{S}_m = -\frac{\varepsilon_0}{4\mu_b \omega i} \mathbf{E} \times \mathbf{E}^* - \frac{\mu_0}{4\varepsilon_b \omega i} \mathbf{H} \times \mathbf{H}^* \quad (6)$$

could have a transverse component in various fields such as a tightly focused Gaussian beam, evanescent field, photonic waveguide, and plasmonic structures, and such a transverse component enables a large number of applications in recent

DOI: 10.1021/acsnano.7b01428
ACS Nano 2017, 11, 4292−4300

years.[37] In the area of optical force, the transverse component of **S** could directly act on chiral particles and give rise to the lateral force.[24,25] In other papers, such a quantity is represented by the chirality flow,[23,38] while their close relations are illustrated by Bliokh *et al.*[28] The relations between the above quantities above are summarized as follows:

$$\bar{\mathbf{P}} = \bar{\mathbf{P}}^{\mathbf{o}} + \bar{\mathbf{P}}^{\mathbf{s}}, \qquad \bar{\mathbf{P}}^{\mathbf{o}} = \bar{\mathbf{P}}^{\mathbf{o}}_{\mathbf{e}} + \bar{\mathbf{P}}^{\mathbf{o}}_{\mathbf{m}}, \qquad \bar{\mathbf{P}}^{\mathbf{s}} = \frac{1}{2}\nabla \times \mathbf{S} \tag{7}$$

Both $\mathbf{F}_{EM}$ and $\mathbf{F}_{INT}$ could be clearly separated into a nonchiral portion (refer to the first four terms of eq 3 and the first two terms of eq 4, respectively) existing for all particles and a chiral portion (refer to the rest of the terms in eqs 3 and 4) existing only for chiral particles. The interference field we consider here consists of two arbitrary polarized plane waves propagating in the $x-z$ plane with an angle 2θ between them, as shown in Figure 2a. The electric field in free space could be written as

$$\mathbf{E}_{1,2} = \frac{A e^{i\varphi_{1,2}}}{\sqrt{1 + |m_{1,2}|^2}}(\cos\theta\hat{x} + m_{1,2}\hat{y} \mp \sin\theta\hat{z}) \tag{8}$$

where φ_1 and φ_1 are the relative phases of the two beams along their propagating directions, $\varphi_{1,2} = k(z\cos\theta \pm x\sin\theta)$, and $\varphi = \varphi_1 - \varphi_2 = 2kx\sin\theta$ stands for the relative phase difference. m_1 and m_2 are two complex numbers describing the polarization states of the waves. The polarization states could also be described by the Stoke parameters T, X, and Σ (their relations with m_1 and m_2 are described in section 2 of the Supporting Information). Substituteing eq 8 into eqs 3 and 4, the optical forces could be derived with details shown in the Methods. The trapping force, radiation pressure, and lateral force are in three orthogonal directions, which is x, z, and y direction, respectively. Among the physical quantities, only the spin part of the momentum $\bar{\mathbf{P}}^{\mathbf{s}}$ and the spin angular momentum **S** have a component in the y direction and result in the lateral force.

Nonzero Lateral Force at the Trapping Position. In the following, we will analyze how the polarization states play an important role in affecting the lateral force and trapping force. First, the case (case A) when the polarizations are completely horizontal or vertical ($m_1 = m_2 = 0/\infty$) is considered.[35] As plotted in Figure 1a, the trapping force only has the nonchiral portion and the lateral force only has the chiral portion. However, these two forces are completely in phase, which makes the lateral force at the trapping positions vanish (refer to Methods and section 4.1 of the Supporting Information for more details).

Such a problem could be solved by simply rotating the polarizations. Assuming the polarizations are still in mirror symmetry but rotated to the diagonal directions (case B) as shown in Figure 2a, such polarization could be described by the Stoke parameter $X = 1$ or $m_1 = 1$ and $m_2 = -1$. In this case, the lateral force and trapping force have both the nonchiral portion and the chiral portion, as plotted in Figure 1b. The chiral portion of force and the nonchiral portion of the force always have a phase difference of $\pi/2$. These two portions superimpose with each other and phase shift the trapping force and the lateral force. After these shifts, the lateral force at the new equilibrium positions is no longer zero.

Figure 2 and Figure 3 quantitatively illustrate how the chirality of the particle affects the optical manipulation. As shown in Figure 2a, when the chirality arises, the lateral force is

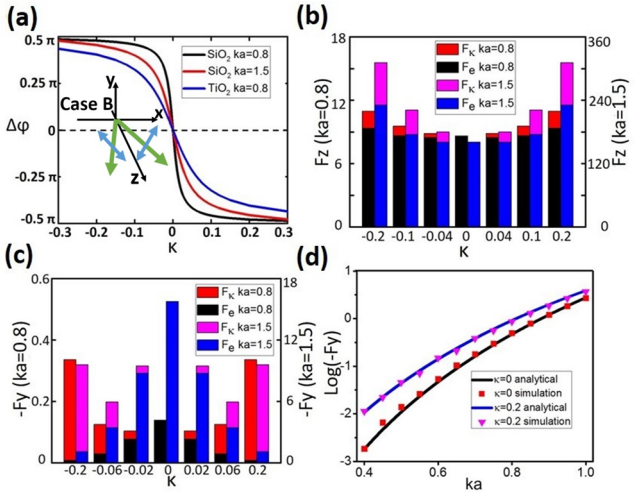

Figure 3. Trapping force and lateral force for case B (schematic plotted in inset of (a)): as can be seen in eqs 12 and 13, the trapping force is always in sinusoidal form. φ is defined as the phase of the trapping force, and $\Delta\varphi$ is defined as the phase shift with respect to nonchiral particles. (a) Phase shift of the trapping force when varying the object's chirality parameter κ. At the trapping position, (b) the radiation pressure F_z and (c) the lateral force F_y when varying the particle's chirality parameter κ. (d) Lateral force in log scale for nonchiral particle ($\kappa = 0$) with $\varepsilon_r = 2.1$ and $u_r = 1$ and chiral particle ($\kappa = 0.2$) with $\varepsilon_r = 2.1$ and $u_r = 1$when varying the particle's size. The forces are also verified by full wave simulations. The incident angle θ is set to 10 degrees.

phase shifted and enhanced in magnitude. The phase shifts first grow dramatically and then saturate to a certain value as the chirality parameter increases (Figure 2b). We attribute the saturation to the fact that the chirality polarizability χ also appears in the nonchiral portion as $|\chi|^2$. The reason for a small particle having a larger saturation value is that the polarizability χ shows a more significant effect on small particles. As the chirality arises, the trapping force is also gradually phase shifted, as shown in Figure 3a. We calculated the lateral forces at the new trapping positons for various particles shown in Figure 3c. We could see the chiral portion of the lateral force at the trapping position takes a higher and higher percentage of the total force as the chirality parameter increases. Although the lateral force may not increase monotonically when the chirality parameter increases, but it will exceed the lateral force on a nonchiral particle when the particle becomes "very chiral".

To verify the above forces numerically, we model the chiral objects as spherical particles made of chiral material. We plotted the lateral force at the trapping position in a logarithmic scale together with the analytically calculated results for a silica particle and a chiral silica particle with $\kappa = 0.2$ in Figure 3d. The simulation results match very well on a chiral particle within the dipole region. Within the region of $ka < 1$ (a is the radius of the particle), one can clearly see that the lateral forces on the particles could be enhanced by up to one order in the presence of chirality.

So far we have demonstrated the nonzero lateral forces at the trapping positions for chiral particles placed in an interference field consisting of two linear polarized plane waves. But simply placing chiral particles in an interference field cannot separate them by their handedness, since the particles with opposite handedness gain lateral force in the same direction, as shown in Figure 3c and section 4.2 of the Supporting Information. When

DOI: 10.1021/acsnano.7b01428
ACS Nano 2017, 11, 4292−4300

the polarization states of two waves are linear (not necessarily in mirror symmetry) or circular at the same time, the lateral forces at the trapping positions are always handedness-insensitive, as illustrated in sections 4.2 and 4.3 of the Supporting Information.

Chiral Separation in an Interference Field. To implement the separation in an interference field, more sophisticated illumination cases have to be investigated. In the following, we consider the case in which one incident beam is linearly polarized and the other one is circularly polarized (case D). Similar to the previous case, the trapping force and the lateral force have both a nonchiral portion and a chiral portion; thus both portions of the trapping force and lateral force are phase shifted when the chirality arises. However, the phase shift of the trapping force is much smaller than that of the lateral force, as shown in Figure 4a. With the help of analytical derived expressions, the explanation of such discrimination is illustrated in the Methods. In this case, the trapping position is relatively fixed, while the lateral force phase is shifted to different directions for chiral particles with opposite handedness (refer to Figure 4b); thus the lateral force at the trapping position receives opposite signs (also refer to section 4.4 of the Supporting Information). The handedness-sensitive lateral forces are plotted for chiral particles with different sizes in Figure 4c. Such forces are also verified by full wave simulation results, which match very well with the analytically derived results. The chiral particles within the dipole range could be separated by placing them in the interference field with such polarization states as shown in Figure 4d.

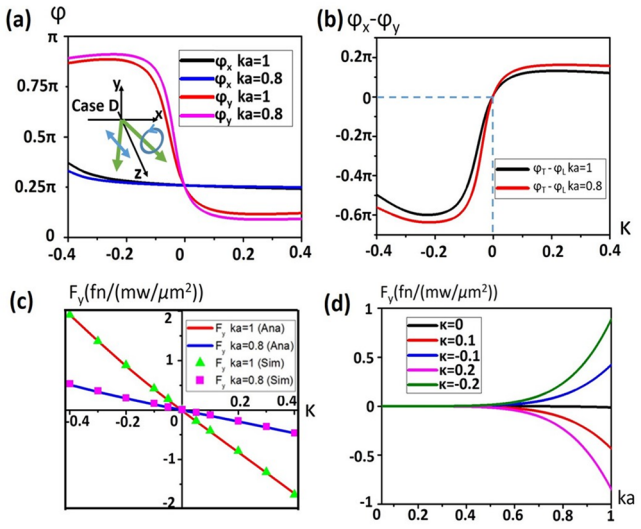

Figure 4. Trapping force and lateral force for case D (schematically plotted in the inset of (a)): as can be seen from eqs 14 and 15, the force in the x and y direction can be written as $F_x = A\sin(\varphi) + B\cos(\varphi) + C$ and $F_y = E\sin(\varphi) + F\cos(\varphi)$, where A, B, C, D, and E are constant. φ_x and φ_y are defined as the phase (φ) when $F_x = 0$ or $F_y = 0$, respectively. φ_x represents the trapping position and φ_y represents the position where the lateral force is zero. (a) Phase of the trapping force (φ_x) and lateral force (φ_y) when varying the object's chirality parameter κ. φ_x is relatively fixed, making the trapping position almost fixed. Since φ_y depends greatly on κ, the lateral force shifts to opposite directions for κ with opposite signs. (b) Phase difference ($\varphi_x - \varphi_y$) of the trapping force and the lateral force. Since the phase difference is zero when $\kappa = 0$, the lateral is zero at the trapping position. When $\varphi - \varphi_y > 0$, the position where $F_y = 0$ shifts to the left of the trapping position; thus the lateral force at the trapping position is negative and *vice versa* (refer to section 4.4 of the Supporting Information). (c) Lateral force F_y at the particle's trapping positions when varying the particle's chirality parameter κ. The forces are also verified by full wave simulations. (d) Lateral force F_y at the particle's trapping positions when varying the particle's size. The incident angle θ is set to 10 degrees. Spherical chiral particles with $\varepsilon_r = 2.1$, $u_r = 1$, and chirality parameter κ are considered.

Chiral Separation with a Single Beam. In the following, we propose an approach to implement the sorting process with a very simple optical setup of a single linear polarized beam taking advantage of the interference field. Tracing back to case A when $T = \pm 1$, although the lateral force has only the chiral portion, it is always zero at the trapping positions. In this case, the spin angular momentum **S** is symmetrically distributed across the trapping position. It is natural to consider introducing a mechanism to break its distribution symmetry. Placing a chiral particle at the interface of two media (Figure 5a) elegantly solves the problem. First, the incident wave and the reflection wave in the incident medium form an interference field that is same as the interference field in case A. However, the presence of the surface breaks the up−down symmetry. The spin angular momentum S in the lateral direction exists only in the upper medium (see black arrows in Figure 6a and b), making its action on the particle nonzero. In addition, the photon momentum is different in different media, which may enhance the lateral force, as will be discussed later.[39,40]

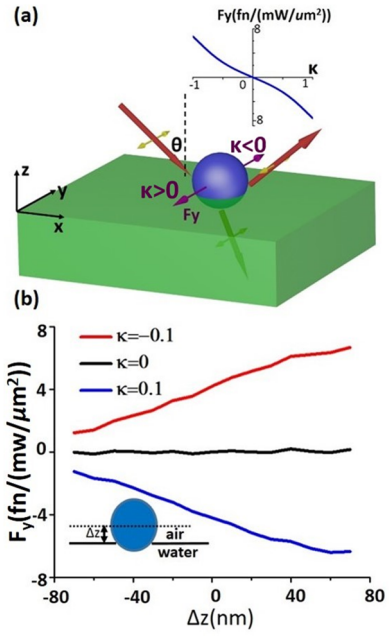

Figure 5. Sorting chiral particles at the interface of two media. (a) A chiral particle is placed at the interface of air and water. Particles with opposite handedness gain lateral forces in opposite directions. 532 nm wavelength light in s-polarization is incident at an angle of 45 deg at the interface of air and water. (b) Lateral force acting on the chiral particle when varying its vertical position z. Chiral particle with $\varepsilon_r = 2.1$ and $u_r = 1$ and characterized by chirality parameter κ in a radius of 100 nm is used in the simulation.

Manipulating objects at the interface of two media is practical in experiments and robust in theory. In our previous works, we have theoretically[40] and experimentally[39] demonstrated optical

DOI: 10.1021/acsnano.7b01428
ACS Nano 2017, 11, 4292−4300

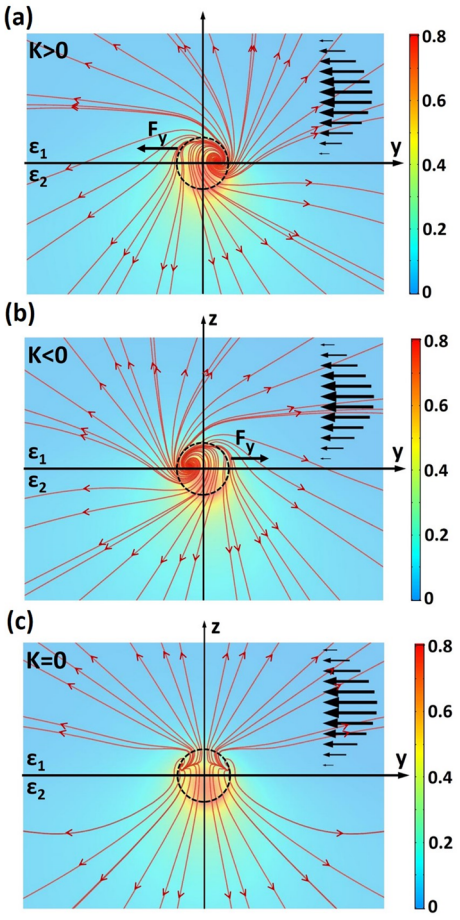

Figure 6. Poynting vector (red line) rotating around the (a) right-handed chiral particle, (b) left-handed chiral particle, and (c) nonchiral particle results in different amounts of energy transferred to the $+y$ and $-y$ directions. The interference field before interacting with the particle formed by the incident and reflection beam generates the spin angular momentum (black arrow) above the interface. Chiral particle with ε_r = 2.1 and u_r = 1 and characterized by chirality parameter κ in a radius of 100 nm is used in the simulation.

tractor beams at the interface of air and water. We have derived the correct methods, which is verified by previous experiments, to calculate the optical force on an object when it is located in inhomogeneous media.[40] A recent work has demonstrated experimentally a lateral force on a polarizable particle placed at the interface of air and water when illuminating circular polarized light on it.[41]

In the following, we will take the example of the sorting of chiral particles at the interface of air and water to illustrate. In general, this method may be applied to any interface of two different media. The situation is shown in Figure 5a: a SiO_2 particle with a radius of 100 nm made of chiral material is placed at the interface of air (n = 1) and water (n = 1.33) when an s-polarized plane wave is illuminated from air at an incident angle θ. The field is derived by the full wave simulation. Then the optical force experienced by the chiral particle is calculated by the integration of the Minkowski stress tensor on a closed surface enclosing the particle. As shown in the inset of Figure 5a, the lateral force in the y direction increasing almost linearly with the chirality of the particle could eventually facilitate the separation of the chiral particles with opposite handedness toward the opposite sides. The lateral force could be easily observed in experiments since the force is of the same order as the force in the beam propagating direction. Figure 5b reports the lateral forces *versus* the vertical displacements Δz of the particle with respect to the interface. The surface energy well at the water−air interface can stably trap the particle in the vertical direction (details discussed in section 7 of the Supporting Information). As long as the particle is at the interface, the lateral force always exists. Our method could also be applied to separate chiral objects within the micrometer scale. The simulation results for sorting 1 μm SiO_2 particles are shown in Section 5 of the Supporting Information.

To interpret this lateral force more intuitively, we show the near-field Poynting vectors in the normal plane (y−z plane) in Figure 6. Comparing with the nonchiral case (Figure 6c), the chiral particle breaks the left−right symmetry in the plane (Figure 6a and b). For a right-handed chiral particle (Figure 6a), most of the energy is scattered to the left[42] in the upper plane (air) and to the right ($+y$) in the lower plane (water). As could be observed in Figure 6, the scattered field is stronger in the lower plane, which makes the scattered energy higher in the lower plane. The existence of different media further enhanced the scattered energy in the lower plane since the phonon momentum is proportional to refractive index of the surrounding medium.[39−41] Now the energy scattered to the right exceeds the energy scattered to the left; thus due to momentum conservation, the particle reverses a recoil force in the left[42] direction. When the left−right symmetry is not broken, the force in the y direction remains zero (Figure 6c). We think that the lateral sorting force could be easily verified in experiments with the proposed configuration.

CONCLUSIONS

In conclusion, we have analytically and numerically demonstrated a solely and passively optical approach to separating chiral objects by optical lateral force taking advantage of the interference field. By properly tailoring the polarization states of two incident beams that form the interference field, we discover nonzero lateral forces sensitive to both the handedness and magnitude of the chirality of the particles at their trapping positions to solve the separating problem. Even with a single beam, the sorting could also be implemented by placing the chiral particles at the interface of two media on which incident and reflected waves naturally interfere. This work investigated chiral light−matter interactions, and the results may be applied to design all-optical approaches for discriminating, manipulating, and studying enantiomer drugs and other chiral substances in the pharmaceutical industries.

METHODS

Analytical Derivation of Optical Force on Chiral Dipoles. In a background medium with the relative permittivity ε_b, permeability μ_b, and refractive index n_b, the time-averaged optical force on a dipole could be calculated by eq 9.[43]

$$\langle \mathbf{F} \rangle = \frac{1}{2}\mathrm{Re}\left[\mathbf{p}(\nabla \otimes \mathbf{E}^*) + \mathbf{m}(\nabla \otimes \mathbf{H}^*) - \frac{ck^4}{6\pi}\frac{1}{\sqrt{\varepsilon_b \mu_b}}(\mathbf{p} \times \mathbf{m}^*)\right] \quad (9)$$

E and H are the incident electric and magnetic field vector, c is the speed of light in free space, and $k = n_b\omega/c$ is the wavenumber. The

DOI: 10.1021/acsnano.7b01428
ACS Nano 2017, 11, 4292−4300

symbol ⊗ represents the dyadic product where $\mathbf{A}(\nabla \otimes \mathbf{B})$ can be written as $\mathbf{A}(\nabla \otimes \mathbf{B}) = (\mathbf{A}\cdot\nabla)\mathbf{B} + \mathbf{A} \times (\nabla \times \mathbf{B})$. Equation 9 calculates the optical force on a small spherical particle within the range of validity of the dipolar approximation. When the size of particle becomes larger, the equation is no longer accurate since higher order modes come into play. The first, second, and third terms in the equation describe the contribution from the electric dipole, the magnetic dipole, and the direct interaction between the electric and magnetic dipoles, respectively. Substituting eq 1 into eq 9 and reorganizing the terms (derived in section 1 of the Supporting Information), the optical force can be written as eqs 2−4. Substituting the optical field eq 8 into eqs 2−4, the detailed expression for the optical force is listed in sections 1 and 2 of the Supporting Information. In the following, we list the optical forces in the x and y directions for the three polarization states (case A, B, and D) discussed in the Results and Discussion, while the force in the z direction is not listed since it is not the focus of the current paper.

Case A: When the polarization stakes are horizontal ($T = 1$ or $m_1 = m_2 = 0$), the optical forces are written as

$$\langle \mathbf{F}_{\mathbf{EM}} \rangle = -\left(\frac{\mathrm{Re}[\alpha_e]}{\varepsilon_0} \cos 2\theta + \frac{\mathrm{Re}[\alpha_m]}{\mu_0} \right) \varepsilon_0 k A^2 \sin\theta \underline{\sin\varphi \hat{x}} \tag{10}$$

$$\langle \mathbf{F}_{\mathbf{INT}} \rangle = \frac{k^4}{6\pi\mu_0} A^2 \sin\theta \, \mathrm{Im}[\alpha_e \alpha_m{}^*] \underline{\sin\varphi \hat{x}} - \frac{ck^4}{6\pi} A^2 \mathrm{Re}[\alpha_e \chi^*] \sin 2\theta \underline{\underline{\sin\varphi \hat{y}}} \tag{11}$$

where the trapping force relying on the terms singly underlined and the lateral force relying on the terms doubly underlined are completely in phase. The lateral force at the trapping position is always zero.

Case B: When the polarization stakes are diagonally mirror symmetric ($X = 1$ or $m_1 = 1$, $m_2 = -1$), the optical forces are written as

$$\langle \mathbf{F}_{\mathbf{EM}} \rangle = \left(\frac{\mathrm{Re}[\alpha_e]}{\varepsilon_0} - \frac{\mathrm{Re}[\alpha_m]}{\mu_0} \right) \varepsilon_0 A^2 k \sin^3\theta \underline{\sin\varphi \hat{x}} + 2\mathrm{Re}[\chi] \varepsilon_0 A^2 \omega \sin\theta \cos^2\theta \underline{\cos\varphi \hat{x}} \tag{12}$$

$$\langle \mathbf{F}_{\mathbf{INT}} \rangle = \frac{k^4 c^2}{6\pi} \varepsilon_0 A^2 (\mathrm{Im}[\alpha_e \alpha_m{}^*] \sin\theta \underline{\sin\varphi \hat{x}} + \frac{1}{2}(\mathrm{Re}[\alpha_e \alpha_m{}^*] + |\chi|^2) \sin 2\theta \underline{\underline{\cos\varphi \hat{y}}} - \frac{1}{2c}\left(\frac{\mathrm{Re}[\alpha_e \chi^*]}{\varepsilon_0} - \frac{\mathrm{Re}[\alpha_m \chi^*]}{\mu_0} \right) \sin 2\theta \underline{\underline{\sin\varphi \hat{y}}}) \tag{13}$$

where the trapping force relying on the terms singly underlined and the lateral force relying on the terms doubly underlined are not completely in phase. The lateral force at the trapping position is nonzero.

Case D: When the polarization stakes are one diagonal linear polarized and the other circular polarized ($m_1 = 1$, $m_2 = \mathrm{i}$), the optical forces are written as

$$\langle \mathbf{F}_{\mathbf{EM}} \rangle = \frac{1}{2} \varepsilon_0 A^2 k \sin\theta \left(\frac{\mathrm{Re}[\alpha_e]}{\varepsilon_0} (\cos\varphi - \cos 2\theta \sin\varphi) + \frac{\mathrm{Re}[\alpha_m]}{\mu_0} (\cos 2\theta \cos\varphi - \sin\varphi) \right) \hat{x} + \varepsilon_0 A^2 \omega \sin\theta (\mathrm{Re}[\chi] \cos^2\theta (\cos\varphi - \sin\varphi) - \mathrm{Im}[\chi]) \hat{x} \tag{14}$$

$$\langle \mathbf{F}_{\mathbf{INT}} \rangle = \frac{c^2 k^4}{12\pi} \varepsilon_0 A^2 (\mathrm{Im}[\alpha_e \alpha_m{}^*] \sin\theta (\sin\varphi + \cos\varphi) \hat{x} - \frac{1}{c} \sin\theta \left(\frac{\mathrm{Re}[\alpha_e \chi^*]}{\varepsilon_0} (\cos\varphi - \sin\varphi - 1) + \frac{\mathrm{Re}[\alpha_m \chi^*]}{\mu_0} (\sin\varphi - \cos\varphi - 1) \right) \hat{x} + \frac{1}{2} (\mathrm{Re}[\alpha_e \alpha_m{}^*] + |\chi|^2 - \mathrm{Im}[\alpha_e \alpha_m{}^*]) \sin 2\theta (\cos\varphi - \sin\varphi) \hat{y} - \frac{1}{c} \sin 2\theta \left(\frac{\mathrm{Re}[\alpha_e \chi^*]}{\varepsilon_0} \sin\varphi - \frac{\mathrm{Re}[\alpha_m \chi^*]}{\mu_0} \cos\varphi \right) \hat{y}) \tag{15}$$

The force in the x and y direction can be written as $F_x = A \sin(\phi) + B \cos(\phi) + C$ and $F_y = E \sin(\phi) + F \cos(\phi)$, where A, B, C, D, and E are independent of ϕ. The period of F_x and F_y are both 2π. ϕ_x and ϕ_y are defined as the phase (ϕ) where $F_x = 0$ or $F_y = 0$, respectively. As plotted in Figure 4a, ϕ_x is relatively independent of the value of the chirality parameter κ. On the other hand, ϕ_y depends greatly on the value of κ. Thus, a chirality-sensitive lateral force is achieved at a relatively fixed trapping position.

Lateral Force Due to the Dual Asymmetry of Matter. The dual asymmetry of matter is also necessary for the chiral portion of lateral force. For case B, the electric and magnetic components of the spin angular momentum in the lateral direction S_e^y and S_m^y are always of the same magnitude and in opposite direction; thus their sum S^y is zero everywhere. For an "ideal" dual-symmetric particle with $\frac{\alpha_e}{\varepsilon_0} = \frac{\alpha_m}{\mu_0}$, the chiral portion of lateral force vanishes since the electric and magnetic components exactly cancel each other. But unlike the dual-symmetric field, the electric polarizability and magnetic polarizability of matter differ significantly. As the whole picture, in the interaction with a chiral particle, the electric and magnetic components of transverse spin angular momentum of the field are converted to the momentum of the particle with different efficiency, and the net momentum leads to the lateral force. As can be seen in eq 13, the dual asymmetry of matter also plays a crucial role in phase shifting the lateral force as chirality arises.

Numerical Simulation of Optical Force. The chiral objects are modeled as spherical particles made of chiral material defined by the constitutive relations.[36]

$$\mathbf{D} = \varepsilon_r \varepsilon_0 \mathbf{E} + \mathrm{i}\kappa/c \mathbf{H}$$
$$\mathbf{B} = -\mathrm{i}\kappa/c \mathbf{E} + u_r u_0 \mathbf{H} \tag{16}$$

ε_r and μ_r are the relative permittivity and permeability of the material. The chirality parameter $\kappa \in [-1, 1]$ is used to describe the chirality of the object. It takes a positive, negative, or zero value for right-handed, left-handed, and nonchiral particles. The electric polarizability α_e, magnetic polarizability α_m, and chiral polarizability χ are complex functions of ε_r, μ_r, and κ. These polarizabilities are derived in Section 3 of the Supporting Information.

In the simulation, the material is set to be silica with $\varepsilon_r = 2.1$ and $\mu_r = 1$. The incident power density is 1 mW/μm^2, and the incident angle θ is set to 10 degrees. The full wave simulation is conducted by FEM methods. Then the optical force is calculated by integrating the Minkowski stress tensor (eq 17) on a closed surface enclosing the entire particle.

$$\langle \bar{\mathbf{T}} \rangle = \frac{1}{2} \mathrm{Re}\left[\mathbf{D} \otimes \mathbf{E}^* + \mathbf{B} \otimes \mathbf{H}^* - \frac{1}{2} \mathbf{I} (\mathbf{E}^* \cdot \mathbf{D} + \mathbf{H}^* \cdot \mathbf{B}) \right] \tag{17}$$

DOI: 10.1021/acsnano.7b01428
ACS Nano 2017, 11, 4292−4300

ASSOCIATED CONTENT

Supporting Information

The Supporting Information is available free of charge on the ACS Publications website at DOI: 10.1021/acsnano.7b01428.

Derivation of optical force on a chiral dipole, expressions of the physics quantities in the force formula, and scattering coefficients of chiral particles in Sections 1−3; examples of lateral force and trapping force in cases A−D in Section 4; in Sections 5 and 6 the chirality sorting at the interface on objects beyond the dipole region and in shapes other than spheres; in Section 7 stability analysis of manipulation at the interface (PDF)

AUTHOR INFORMATION

Corresponding Author

*E-mail: chengwei.qiu@nus.edu.sg.

ORCID

Tianhang Zhang: 0000-0002-7939-5302
Mahdy Rahman Chowdhury Mahdy: 0000-0003-3737-0315
Jing Hua Teng: 0000-0001-5331-3092
Cheng-Wei Qiu: 0000-0002-6605-500X

Notes

The authors declare no competing financial interest.

ACKNOWLEDGMENTS

T.Z. acknowledges the scholarship from NUS Graduate School for Integrative Sciences and Engineering (NGS). C.T.L. acknowledges support by the National Research Foundation, Prime Minister's Office, Singapore, under its Research Centre of Excellence, Mechanobiology Institute.

REFERENCES

(1) Ashkin, A.; Dziedzic, J. M.; Bjorkholm, J. E.; Chu, S. Observation of a Single-Beam Gradient Force Optical Trap for Dielectric Particles. *Opt. Lett.* **1986**, *11*, 288−290.

(2) Ashkin, A.; Dziedzic, J.; Yamane, T. Optical Trapping and Manipulation of Single Cells Using Infrared Laser Beams. *Nature* **1987**, *330*, 769−771.

(3) Cecconi, C.; Shank, E. A.; Bustamante, C.; Marqusee, S. Direct Observation of the Three-State Folding of a Single Protein Molecule. *Science* **2005**, *309*, 2057−2060.

(4) Wen, J.-D.; Lancaster, L.; Hodges, C.; Zeri, A.-C.; Yoshimura, S. H.; Noller, H. F.; Bustamante, C.; Tinoco, I. Following Translation by Single Ribosomes One Codon at a Time. *Nature* **2008**, *452*, 598−603.

(5) Crocker, J.; Matteo, J.; Dinsmore, A.; Yodh, A. Entropic Attraction and Repulsion in Binary Colloids Probed with a Line Optical Tweezer. *Phys. Rev. Lett.* **1999**, *82*, 4352.

(6) Li, H.; Zhou, D.; Browne, H.; Klenerman, D. Evidence for Resonance Optical Trapping of Individual Fluorophore-Labeled Antibodies Using Single Molecule Fluorescence Spectroscopy. *J. Am. Chem. Soc.* **2006**, *128*, 5711−5717.

(7) Chang, D.; Thompson, J.; Park, H.; Vuletić, V.; Zibrov, A.; Zoller, P.; Lukin, M. Trapping and Manipulation of Isolated Atoms Using Nanoscale Plasmonic Structures. *Phys. Rev. Lett.* **2009**, *103*, 123004.

(8) Reiserer, A.; Nölleke, C.; Ritter, S.; Rempe, G. Ground-State Cooling of a Single Atom at the Center of an Optical Cavity. *Phys. Rev. Lett.* **2013**, *110*, 223003.

(9) Liu, M.; Zentgraf, T.; Liu, Y.; Bartal, G.; Zhang, X. Light-Driven Nanoscale Plasmonic Motors. *Nat. Nanotechnol.* **2010**, *5*, 570−573.

(10) Roxworthy, B. J.; Ko, K. D.; Kumar, A.; Fung, K. H.; Chow, E. K.; Liu, G. L.; Fang, N. X.; Toussaint, K. C., Jr. Application of Plasmonic Bowtie Nanoantenna Arrays for Optical Trapping, Stacking, and Sorting. *Nano Lett.* **2012**, *12*, 796−801.

(11) Allen, L.; Barnett, S. M.; Padgett, M. J. *Optical Angular Momentum*; Taylor & Francis, 2003.

(12) Novitsky, A.; Qiu, C. W.; Wang, H. F. Single Gradientless Light Beam Drags Particles as Tractor Beams. *Phys. Rev. Lett.* **2011**, *107*, 203601.

(13) Chen, J.; Ng, J.; Lin, Z. F.; Chan, C. T. Optical Pulling Force. *Nat. Photonics* **2011**, *5*, 531−534.

(14) Sukhov, S.; Dogariu, A. Negative Nonconservative Forces: Optical "Tractor Beams" for Arbitrary Objects. *Phys. Rev. Lett.* **2011**, *107*, 203602.

(15) Brzobohaty, O.; Karasek, V.; Siler, M.; Chvatal, L.; Cizmar, T.; Zemanek, P. Experimental Demonstration of Optical Transport, Sorting and Self-Arrangement Using a 'Tractor Beam'. *Nat. Photonics* **2013**, *7*, 254−254.

(16) Dogariu, A.; Sukhov, S.; Sáenz, J. Optically Induced 'Negative Forces'. *Nat. Photonics* **2013**, *7*, 24−27.

(17) Bliokh, K. Y.; Bekshaev, A. Y.; Nori, F. Extraordinary Momentum and Spin in Evanescent Waves. *Nat. Commun.* **2014**, *5*, 3300.

(18) Bekshaev, A. Y.; Bliokh, K. Y.; Nori, F. Transverse Spin and Momentum in Two-Wave Interference. *Phys. Rev. X* **2015**, *5*, 011039.

(19) Sekhon, B. S. Chiral Pesticides. *J. Pestic. Sci.* **2009**, *34*, 1−12.

(20) Abate, A.; Brenna, E.; Fuganti, C.; Gatti, F. G.; Serra, S. Odor and (Bio) Diversity: Single Enantiomers of Chiral Fragrant Substances. *Chem. Biodiversity* **2004**, *1*, 1888−1898.

(21) Nguyen, L. A.; He, H.; Pham-Huy, C. Chiral Drugs: An Overview. *International journal of biomedical science: IJBS* **2006**, *2*, 85−100.

(22) Stalcup, A. M., Chiral Separations. *Kirk-Othmer Encyclopedia of Chemical Technology* **2010** 10.1002/0471238961.0308091819200112.a01.

(23) Antoine, C.-D.; James, A. H.; Cyriaque, G.; Thomas, W. E. Mechanical Separation of Chiral Dipoles by Chiral Light. *New J. Phys.* **2013**, *15*, 123037.

(24) Wang, S. B.; Chan, C. T. Lateral Optical Force on Chiral Particles near a Surface. *Nat. Commun.* **2014**, *5*, 3307.

(25) Hayat, A.; Mueller, J. P. B.; Capasso, F. Lateral Chirality-Sorting Optical Forces. *Proc. Natl. Acad. Sci. U. S. A.* **2015**, *112*, 13190−13194.

(26) Tkachenko, G.; Brasselet, E. Optofluidic Sorting of Material Chirality by Chiral Light. *Nat. Commun.* **2014**, *5*, 3577.

(27) Bliokh, K. Y.; Alonso, M. A.; Ostrovskaya, E. A.; Aiello, A. Angular Momenta and Spin-Orbit Interaction of Nonparaxial Light in Free Space. *Phys. Rev. A: At., Mol., Opt. Phys.* **2010**, *82*, 063825.

(28) Bliokh, K. Y.; Nori, F. Characterizing Optical Chirality. *Phys. Rev. A: At., Mol., Opt. Phys.* **2011**, *83*, 021803.

(29) Liu, X.; Chern, R.; Tsai, D. A Study of Optical Properties of Chiral Metamaterials. *Optics Engineering* **2009**, 23−31.

(30) Gao, W.; Lawrence, M.; Yang, B.; Liu, F.; Fang, F.; Béri, B.; Li, J.; Zhang, S. Topological Photonic Phase in Chiral Hyperbolic Metamaterials. *Phys. Rev. Lett.* **2015**, *114*, 037402.

(31) Hou, Y.; Leung, H. M.; Chan, C. T.; Du, J.; Chan, H. L. W.; Lei, D. Y. Ultrabroadband Optical Superchirality in a 3d Stacked-Patch Plasmonic Metamaterial Designed by Two-Step Glancing Angle Deposition. *Adv. Funct. Mater.* **2016**, *26*, 7807−7816.

(32) Tang, Y.; Cohen, A. E. Enhanced Enantioselectivity in Excitation of Chiral Molecules by Superchiral Light. *Science* **2011**, *332*, 333−336.

(33) Bao, Z. Y.; Zhang, W.; Zhang, Y. L.; He, J.; Dai, J.; Yeung, C. T.; Law, G. L.; Lei, D. Y. Interband Absorption Enhanced Optical Activity in Discrete Au@ Ag Core−Shell Nanocuboids: Probing Extended Helical Conformation of Chemisorbed Cysteine Molecules. *Angew. Chem., Int. Ed.* **2017**, *56*, 1283−1288.

(34) Zhao, Y.; Askarpour, A. N.; Sun, L.; Shi, J.; Li, X.; Alù, A. Chirality Detection of Enantiomers Using Twisted Optical Metamaterials. *Nat. Commun.* **2017**, *8*, 14180.

(35) Chen, H.; Liang, C.; Liu, S.; Lin, Z. Chirality Sorting Using Two-Wave-Interference Induced Lateral Optical Force. *Phys. Rev. A: At., Mol., Opt. Phys.* **2016**, *93*, 053833.

(36) Bohren, C. F.; Huffman, D. R. *Absorption and Scattering of Light by Small Particles*; John Wiley & Sons, 2008.

DOI: 10.1021/acsnano.7b01428
ACS Nano 2017, 11, 4292−4300

(37) Aiello, A.; Banzer, P.; Neugebauer, M.; Leuchs, G. From Transverse Angular Momentum to Photonic Wheels. *Nat. Photonics* **2015**, *9*, 789−795.
(38) Tang, Y.; Cohen, A. E. Optical Chirality and Its Interaction with Matter. *Phys. Rev. Lett.* **2010**, *104*, 163901.
(39) Kajorndejnukul, V.; Ding, W. Q.; Sukhov, S.; Qiu, C. W.; Dogariu, A. Linear Momentum Increase and Negative Optical Forces at Dielectric Interface. *Nat. Photonics* **2013**, *7*, 787−790.
(40) Qiu, C.-W.; Ding, W.; Mahdy, M.; Gao, D.; Zhang, T.; Cheong, F. C.; Dogariu, A.; Wang, Z.; Lim, C. T. Photon Momentum Transfer in Inhomogeneous Dielectric Mixtures and Induced Tractor Beams. *Light: Sci. Appl.* **2015**, *4*, e278.
(41) Sukhov, S.; Kajorndejnukul, V.; Naraghi, R. R.; Dogariu, A. Dynamic Consequences of Optical Spin-Orbit Interaction. *Nat. Photonics* **2015**, *9*, 809−812.
(42) Hsu, L.-C.; Chen, T.-C.; Yang, Y.-T.; Huang, C.-Y.; Shen, D.-W.; Chen, Y.-T.; Lee, M.-C. M. Manipulation of Micro-Particles through Optical Interference Patterns Generated by Integrated Photonic Devices. *Lab Chip* **2013**, *13*, 1151−1155.
(43) Nieto-Vesperinas, M.; Saenz, J. J.; Gomez-Medina, R.; Chantada, L. Optical Forces on Small Magnetodielectric Particles. *Opt. Express* **2010**, *18*, 11428−11443.

DOI: 10.1021/acsnano.7b01428
ACS Nano 2017, 11, 4292−4300